THE FASEB JOURNAL • RESEARCH • www.fasebj.org

Stress hormone signaling through β-adrenergic receptors regulates macrophage mechanotype and function

Tae-Hyung Kim,[*,†] Chau Ly,[*,‡] Alexei Christodoulides,[*] Cameron J. Nowell,[§] Peter W. Gunning,[¶] Erica K. Sloan,[†,§,‖,#,,1,2] and Amy C. Rowat[*,‡,#,1,3]**

[*]Department of Integrative Biology and Physiology, [†]Cousins Center for Psychoneuroimmunology, Semel Institute for Neuroscience and Human Behavior, [‡]Department of Bioengineering, [#]UCLA Jonsson Comprehensive Cancer Center, and **UCLA AIDS Institute, University of California, Los Angeles, California, USA; [§]Drug Discovery Biology Theme, Monash Institute of Pharmaceutical Sciences, Monash University, Parkville, Victoria, Australia; [¶]School of Medical Sciences, University of New South Wales Sydney, Kensington, New South Wales, Australia; and [‖]Division of Cancer Surgery, Peter MacCallum Cancer Centre, Melbourne, Victoria, Australia

ABSTRACT: Critical functions of immune cells require them to rapidly change their shape and generate forces in response to cues from their surrounding environment. However, little is known about how soluble factors that may be present in the microenvironment modulate key aspects of cellular mechanobiology—such as immune cell deformability and force generation—to impact functions such as phagocytosis and migration. Here we show that signaling by soluble stress hormones through β-adrenoceptors (β-AR) reduces the deformability of macrophages; this is dependent on changes in the organization of the actin cytoskeleton and is associated with functional changes in phagocytosis and migration. Pharmacologic interventions reveal that the impact of β-AR signaling on macrophage deformability is dependent on actin-related proteins 2/3, indicating that stress hormone signaling through β-AR shifts actin organization to favor branched structures rather than linear unbranched actin filaments. These findings show that through remodeling of the actin cytoskeleton, β-AR-mediated stress hormone signaling modulates macrophage mechanotype to impact functions that play a critical role in immune response.—Kim, T.-H., Ly, C., Christodoulides, A., Nowell, C. J., Gunning, P. W., Sloan, E. K., Rowat, A. C. Stress hormone signaling through β-adrenergic receptors regulates macrophage mechanotype and function. FASEB J. 33, 3997–4006 (2019). www.fasebj.org

KEY WORDS: deformability · phagocytosis · chemotaxis · actin

Immune cells sense and integrate information from diverse environmental cues (1–3). In response to physiologic and psychologic stressors, fibers of the peripheral sympathetic nervous system release catecholaminergic stress hormones including norepinephrine into major organ systems to induce a "fight-or-flight" response; epinephrine is released from the adrenal gland into circulation (4, 5). Norepinephrine and epinephrine bind to β-adrenergic receptors (β-ARs) to mediate changes in immune cell function. Such neuroendocrine-immune communication is evolutionarily conserved (6) and critical for modulating immune response [reviewed in (7)]. Macrophages are essential for immune function: inflammation triggers blood-circulating monocytes to be recruited and differentiate into macrophages (8). Resident macrophages are present in major organs and perform crucial functions in tissue homeostasis, such as eliminating infectious agents, mediating inflammation, and repairing tissue damage (9–11). β-AR signaling induces molecular changes in macrophages, including up-regulation of immune receptor CD14 and increased secretion of cytokines including TNF-α, IL-6, and IL-10 (12–14), as well as changes in integrin affinity (15). β-AR signaling has also been shown to affect phagocytosis, but studies reveal inconsistent results (13, 15). However, despite the importance of stress hormones in modulating immune cell function, little is understood about the physical and molecular mechanisms that underlie β-AR regulation of macrophage functions including migration and phagocytosis.

ABBREVIATIONS: APC, antigen presenting cell; β-AR, β-adrenergic receptor; Arp2/3, actin-related protein 2/3; FBS, fetal bovine serum; PMA, phorbol 12-myristate 13-acetate; PMF, parallel microfiltration; qRT-PCR, quantitative RT-PCR; TT, transit time

[1] These authors contributed equally to this work.

[2] Correspondence: Monash Institute of Pharmaceutical Sciences, 381 Royal Parade, Parkville, VIC 3052, Australia. E-mail: erica.sloan@monash.edu

[3] Correspondence: UCLA, Terasaki Life Sciences Building 1125, 610 Charles E Young Dr. South, Los Angeles, CA 90095, USA. E-mail: rowat@ucla.edu

doi: 10.1096/fj.201801429RR

This article includes supplemental data. Please visit *http://www.fasebj.org* to obtain this information.

The mechanical phenotype—or mechanotype—of macrophages is intimately linked to their function (16, 17). The compliance of macrophages has been associated with their advection through narrow channels and migration through micron-scale pores (18). Macrophage phagocytosis has also been associated with cell mechanical properties (19). The link between mechanotype and functions can be explained as phagocytosis and migration require force generation and changes in cellular shape, which are regulated by shared molecular mediators. A primary determinant of the mechanical stability of macrophages is the actin cytoskeleton, which also provides critical force-generating machinery for the cell (18, 20). Protrusions and cellular shape changes generated by actin polymerization and branching—which are mediated by the actin-related protein 2/3 (Arp2/3) complex and formins—are required for functions such as migration and phagocytosis (21–24). However, it is poorly defined how stress hormone signaling modulates actin organization and dynamics to regulate macrophage mechanical properties and function. Such knowledge would provide mechanistic insight into how cells alter their physical properties in response to a soluble physiologic cue.

Here we investigate how β-AR signaling modulates macrophage mechanotype and key functions of phagocytosis and migration. Using U937 human myeloid cells and RAW 264.7 mouse myeloid cells, we show that signaling through β-AR reduces the deformability of differentiated macrophages but not of precursor monocytes. β-AR regulation of cell deformability is dependent on remodeling of the actin cytoskeleton and is associated with changes in phagocytosis and migration. These findings show that β-AR signaling, which is activated by soluble stress hormones, induces changes in macrophage mechanotype and critical functions of phagocytosis and migration. To our knowledge, this is the first report of how a physiologic cue regulates cellular physical phenotype and physiologic functions by shifting the balance between branched and unbranched actin filament populations.

MATERIALS AND METHODS

Cells and reagents

The human histomonocytic (U937) cell line [American Type Culture Collection (ATCC), Manassas, VA, USA] was maintained in RPMI 1640 media supplemented with 10% fetal bovine serum (FBS; Gemini Bio-Products, West Sacramento, CA, USA) and 1% penicillin and streptomycin (Thermo Fisher Scientific, Waltham, MA, USA). Macrophage-like cells were differentiated by treatment with 50 ng/ml phorbol 12-myristate 13-acetate (PMA) in serum-free medium for 24 h (25). The murine macrophage (RAW 264.7) cell line (ATCC) was maintained in DMEM (Thermo Fisher Scientific) supplemented with 10% FBS and 1% penicillin and streptomycin (Thermo Fisher Scientific). All cells were maintained at 37°C, 5% CO_2.

The β-AR agonist (isoproterenol) and antagonist (propranolol) were from MilliporeSigma (Burlington, MA, USA). The adenylyl cyclase activator forskolin (MilliporeSigma) was used at 10 μM for 24 h. To inhibit polymerization of F-actin, we treated cells with 2 μM cytochalasin D (Santa Cruz Biotechnology, Dallas, TX, USA) for 1 h. To inhibit the activity of Arp2/3 and formins, cells were treated with 50 μM CK666 (MilliporeSigma) or 20 μM SMIFH2 (MilliporeSigma) for 24 h. To chelate intracellular Ca^{2+}, cells were treated with 10 μM 1,2-bis(2-aminophenoxy)ethane-*N*,*N*,*N*′,*N*′-tetraacetic acid tetrakis-acetoxymethyl ester (Thermo Fisher Scientific) for 24 h.

Quantitative RT-PCR

To measure levels of β-adrenoceptors in U937 cells before and after PMA-differentiation into macrophages, TRIzol reagent (Thermo Fisher Scientific) was used to extract total RNA from cells according to the manufacturer's protocol. cDNA was obtained using SuperScript III First-Strand Synthesis System (Thermo Fisher Scientific) starting from 1 μg of RNA. Quantitative PCR was performed using the CFX96 Touch Real-Time PCR Detection System (Bio-Rad, Hercules, CA, USA) and SYBR Green Real-Time PCR Master Mixes (Thermo Fisher Scientific) with the following primers: GAPDH (forward: 5′-tgcaccaccaactgcttagc-3′, reverse: 5′-ggcatggactgtggtcatgag-3′), TLR4 (forward: 5′-agacctgtccctgaaccctat-3′, reverse: 5′-cgatggacttctaaaccagcca-3′), CCR2 (forward: 5′-ccacatctcgttctcggtttatc-3′, reverse: 5′-cagggagcaccgtaatcataatc-3′), CD14 (forward: 5′-acgccagaaccttgtgagc-3′, reverse: 5′-gcatggatctccacctctactg-3′), CD163 (forward: 5′-tttgtcaacttgagtcccttcac-3′, reverse: 5′-tcccgctacacttgttttcac-3′), CSF1R (forward: 5′-gggaatcccagtgatagagcc-3′, reverse: 5′-ttggaaggtagcgttgttggt-3′), CD68 (forward: 5′-cttctctcattcccctatggaca-3′, reverse: 5′-gaaggacacattgtactccacc-3′), CD16/FCGR3A (forward: 5′-cctcctgtctagtcggtttgg-3′, reverse: 5′-tcgagcaccctgtaccattga-3′), CD71/TFRC (forward: 5′-accattgtcatatacccggttca-3′, reverse: 5′-caatagcccaagtagccaatcat-3′).

Flow cytometry

To confirm differentiation of U937 cells, we quantified the canonical macrophage surface marker, CD11b. Differentiated and undifferentiated U937 cells were harvested in ice-cold PBS containing 10% FBS solution. We then immunolabeled 1×10^6 cells with 0.75 μg of phycoerythrin-conjugated CD11b antibody (301306; BioLegend, San Diego, CA, USA) for 30 min at room temperature. After being washed with PBS, cells were analyzed with FACSAria II High-Speed Cell Sorter with FACSDiva software (BD Biosciences, San Jose, CA, USA) and FlowJo software (FlowJo, Ashland, Oregon, USA) at the University of California, Los Angeles (UCLA) Broad Stem Cell Research Center Flow Cytometry Core. To measure β_2AR expression levels, we fixed cells with 4% paraformaldehyde and labeled them with 0.60 μg of FITC-conjugated β_2AR antibody (sc-271322; Santa Cruz Biotechnology) before analyzing by flow cytometry.

Phagocytosis assay

To quantify phagocytosis, we measured the uptake of pH-sensitive dye (pHrodo) conjugated *E. coli* bioparticles (26) into macrophages using an automated live cell imaging system (IncuCyte Zoom; Essen BioScience, Ann Arbor, MI, USA) (27). Because the fluorescence of the pHrodo dye conjugated to *E.coli* bioparticles is sensitive to pH, the fluorescence increases once the particles are internalized through phagocytosis. PMA-differentiated U937 cells were treated with forskolin (10 μM) or isoproterenol (100 nM) with or without inhibitors of actin polymerization, branching, and nucleation (2 μM cytochalasin D, 50 μM CK666, and 20 μM SMIFH2). After 1 h of incubation, 10 μg/well of pHrodo conjugated *E. coli* bioparticles (Thermo Fisher Scientific) were added, and images were then acquired every 2 h for 48 h. To quantify the total green object area (square micrometers per image), which indicates the number of internalized

particles, images were analyzed using IncuCyte Zoom software (Essen BioScience).

Chemotaxis assay

Chemotaxis of macrophages was measured using a transwell migration assay. We seeded 8×10^5 U937 cells on polycarbonate membranes with 5 μm-diameter pores (Transwell Inserts; Corning, Corning, NY, USA) and differentiated cells as previously described. After 24 h, forskolin (10 μM), propranolol (10 μM), or isoproterenol (100 nM) with or without other actin-perturbing drugs were added in both upper inserts and lower wells. To induce chemotaxis, the chemoattractant, 10% FBS, was added only to the lower wells. After incubation for 6 h at 37°C, we determined the number of cells that had migrated through to the lower well by staining the remaining cells in the lower well with Hoechst 33342 (10 μg/ml) for 30 min at room temperature. To quantify chemotaxis efficacy, we counted the number of cells that migrated into the lower well by acquiring at least 5 images per well using a charge-coupled device camera (AxioCam MRm; Carl Zeiss, Oberkochen, Germany) mounted on an inverted fluorescence microscope (Carl Zeiss) with ×10 objective (Zeiss EC Plan-NEOFLUAR, NA:0.3) equipped with X-Cite 120Q light source.

Quantitative image analysis

To quantify levels of F-actin, 1×10^6 undifferentiated U937 cells were plated on a glass (Millicell Ez Slides; MilliporeSigma) coated with 100 μg/ml of Matrigel (Corning) followed by differentiation with PMA. To identify single cells, we labeled both F-actin (phalloidin) and DNA (DRAQ5). Cells were fixed with 4% paraformaldehyde for 15 min at room temperature, and then incubated for 1 h at room temperature with phalloidin (Alexa Fluor 546-conjugated Phalloidin, 1:200; Thermo Fisher Scientific) and DRAQ5 (1:1000; Thermo Fisher Scientific) diluted in 1% (w/v) bovine serum albumin in PBS with 0.3% Triton X-100. To acquire images, we used a laser-scanning confocal microscope (LSM 5; Carl Zeiss) equipped with argon (488 and 514 nm), HeNe (543 nm), and Red Diode (633 nm) lasers, and a ×63 objective (NA1.2 W Corr UV-VIS-IR, C-Apochromat; Carl Zeiss). For quantification of F-actin levels, we used a custom script to perform watershed segmentation and extract cell regions to measure actin intensity per cell (ImageJ; National Institutes of Health, Bethesda, MD, USA) (28).

Parallel microfiltration

To measure the deformability of cells, which is indicated by their ability to filter through 5 μm pores of a membrane with applied pressure, we used parallel microfiltration (PMF) as described in our previous studies (29, 30). Briefly, cells were treated with drugs for 24 h, and we prepared a suspension of single cells by trypsin treatment for 3 min followed by scraping to harvest additional cells that remain adhered. Cells were counted (TC20; Bio-Rad) to generate a suspension of 5×10^5 cells in culture media, which is placed in a well of the PMF device. To drive the cell suspension to pass through the 5 μm pore-polycarbonate membrane, we applied an air pressure of 2.0 kPa for 30 s. Retention was determined by measuring the mass of the cell suspension that was retained at the end of the filtration timecourse compared with the initial mass loaded ($mass_{final}/mass_{initial}$). Higher retention indicates a population of cells that has a higher probability to occlude pores compared with a suspension of cells that more readily transit through pores. Cells with higher elastic modulus as measured by atomic force microscopy tend to have a higher probability of occluding micron-scale pores (31, 32).

Quantitative deformability cytometry

To measure the deformability of single cells, we used quantitative deformability cytometry as described in our previous studies (31, 33). Briefly, cell suspensions were flowed through polydimethylsiloxane (PDMS) microfluidic devices with channels that were 5 μm × 10 μm (width × height); the timescale of cell transit, or transit time, provides a measure of cell deformability (34). We flowed suspensions of 1.5×10^6 cells/ml through q-DC devices using a driving pressure of 41 kPa and captured 2500 frames/sec using a CMOS camera (Phantom) mounted on an inverted microscope (Carl Zeiss) equipped with a ×20/0.40 NA objective. We performed post acquisition analysis using Matlab (MathWorks, Natick, MA, USA) to determine the transit time for individual cells (*https://github.com/knybe/RowatLab-DC-Analysis*).

Statistical analyses

All experiments were performed at least 3 independent times. Statistical significance between control and treated groups was determined with an unpaired *t* test or 1-way ANOVA with Tukey's multiple comparison *post hoc* analysis using Graphpad Prism 5 (GraphPad Software, La Jolla, CA, USA).

RESULTS

β-AR signaling reduces the deformability of macrophages

To determine whether β-AR signaling drives physical changes in myeloid cells, we examined the effect of the β-AR agonist isoproterenol on the deformability of monocytes and macrophages. First we investigated the human U937 monocyte cell line that can be differentiated into macrophage-like cells by treatment with PMA (35, 36). PMA-differentiated U937 cells have been widely used as a model for macrophages because they express macrophage marker proteins and exhibit similar behaviors to macrophages including phagocytosis and chemotaxis (37–39). Differentiation of U937 cells into macrophage-like cells following PMA treatment was confirmed by the up-regulated transcription of key macrophage markers including *CD14*, *CSF1R*, and *CD163* determined by quantitative RT-PCR (qRT-PCR) and the increased surface expression of *CD11b* measured by flow cytometry (Supplemental Fig. S1*A–D*). Using qRT-PCR, we confirmed that both precursor monocytes (undifferentiated U937 cells) and macrophages (PMA-treated U937 cells) express the β-AR subtypes, *ADRB1*, *ADRB2*, and *ADRB3* (Supplemental Fig. S1*E*). To determine effects of β-AR activation on both monocyte and macrophage physical properties, we treated cells with isoproterenol and measured their ability to deform through micron-scale pores using PMF (29, 30). In this assay, air pressure is applied to drive a suspension of cells through 5 μm diameter pores over a relatively short timescale of 30 s, and the volume of fluid retained above the membrane is determined; the retention volume depends on the number of pores that have

been occluded by cells, which is largely determined by the physical properties of cells, including cell size and deformability (29). Before filtration, cells were treated with isoproterenol across a range of concentrations from 1 to 100 nM, which have been shown to induce intracellular signaling and invasion of cancer cells (40, 41). We found that isoproterenol had no effect on the retention of monocytes (**Fig. 1*A***), suggesting that β-AR signaling does not change monocyte physical properties. By contrast, we observed a significant increase in retention of macrophages with increasing isoproterenol dose, suggesting β-AR signaling changes macrophage physical properties in a concentration-dependent manner (Fig. 1*A*). We found no significant changes in cell size distributions with or without isoproterenol (Fig. 1*B*), suggesting that increased retention of macrophages with β-AR signaling is due to decreased cell deformability. To determine whether the differential effect of β-AR signaling in monocytes and macrophages resulted from different levels of β-AR, we used flow cytometry to measure surface levels of β_2AR, which is the dominant β-AR subtype in myeloid cells (14). We found no significant differences in β_2AR levels in U937 cells before and after PMA treatment (Supplemental Fig. S1*F–H*). Nor did we find any difference in levels of *ADRB2* transcripts measured by qRT-PCR (Supplemental Fig. S1*E*). Taken together, these data indicate that stress hormone signaling through β-AR selectively modulates the mechanotype of macrophages.

To validate the β-AR–induced changes in deformability using an independent method, we used quantitative deformability cytometry to measure the timescale for individual macrophages to transit through 5 μm constrictions in a microfluidic device (31, 33); cells that are stiffer have longer transit times (33). Activation of β-AR signaling increased the transit time (TT) of macrophages (median TT_{Veh} *vs.* TT_{Iso}: 6.9 *vs.* 9.4 ms, $P < 0.0001$) (Fig. 1*C*, *D*), consistent with findings by PMF that cells are becoming less deformable with β-AR activation. To investigate whether the β-AR–induced changes in cell deformability are generalizable to other myeloid cells, we measured the retention of the mouse macrophage cell line RAW 264.7 following treatment with the β-AR agonist isoproterenol. Consistent with findings for U937-derived macrophages, β-AR activation resulted in increased retention of RAW 264.7 cells, indicating a concentration-dependent reduction in cellular deformability (Fig. 1*E*); we note that a slight increase in deformability was observed for 1 nM of isoproterenol treatment, which is not seen in the human

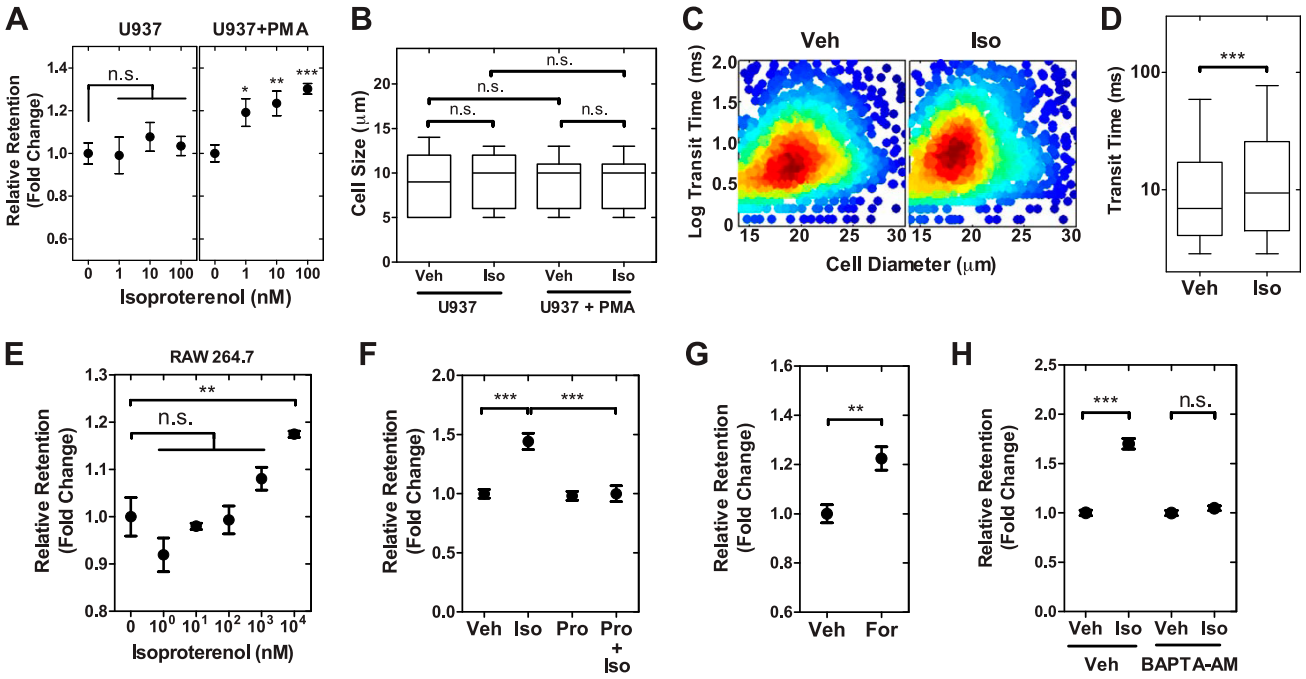

Figure 1. β-AR signaling activation reduces the deformability of macrophages. *A*) Retention of monocyte (U937) and macrophage (U937+PMA) cells was measured using parallel microfiltration after isoproterenol treatment for 24 h. Retention is measured by the mass of cell suspension that remains in the top well after applying 2 kPa pressure for 30 s relative to the initial mass. Higher retention indicates that cells are more likely to occlude the 5 μm pores. *B*) Cell size distribution of monocytes and macrophages in vehicle control (Veh) and isoproterenol (Iso)-treated groups. *C*) Density scatterplot shows data from quantitative deformability cytometry. We measure cell size and transit time, or the timescale for macrophages to pass through the 5 × 10 μm gap of a microfluidic channel ($n > 1600$). *D*) Boxplot shows the lower and upper quartiles with median (line). Whiskers show the 10–90th percentiles ($P < 0.0001$). *E*) Isoproterenol effects on mouse macrophage (RAW 264.7) cells. *F–H*) Relative retention measured by PMF following 24 h treatment with Iso (100 nM) and the β-blocker propranolol (Pro) (10 μM) (*F*). Pro+Iso indicates cotreatment. Adenylyl cyclase activator forskolin (For; 10 μM) (*G*). Calcium chelator BAPTA-AM [1,2-Bis (2-aminophenoxy)ethane-*N*,*N*,*N*′,*N*′-tetraacetic acid tetrakis-acetoxymethyl ester] (10 μM) (*H*). One-way ANOVA test with Tukey's multiple comparison test. $^*P < 0.05$, $^{**}P < 0.01$, $^{***}P < 0.001$; n.s., not significant. Results represent data from at least 3 independent experiments ($N = 3$).

U937 cell line. Although the trend of increased retention with isoproterenol treatment was consistent across both human and mouse cells, the increase in retention for the mouse cells occurred at a higher isoproterenol concentration (~1000 nM) compared with the human cells (~1 nM), consistent with the lower expression of *Adrb2* in RAW 264.7 cells (42).

To determine whether the effects of isoproterenol on macrophage deformability are modulated by signaling through β-AR—rather than nonspecific off-target effects—we treated cells with the β-AR antagonist propranolol to compete binding of the β-AR agonist at the receptor. We found that propranolol itself does not modulate cell deformability (P = 0.73; Fig. 1*F*), but propranolol blocked the increased retention with isoproterenol, confirming that signaling through β-AR mediates the effects on macrophage deformability (Fig. 1*F*). To identify the downstream signaling pathway that regulates cellular deformability, we manipulated other mediators downstream in the β-AR signaling pathway (41). β-AR is a $G\alpha_s$-protein coupled receptor that activates adenylyl cyclase to elevate levels of intracellular cAMP and calcium (32, 41). To directly activate adenylyl cyclase, we treated U937 macrophages with forskolin and found increased retention, consistent with reduced deformability (Fig. 1*G*). To determine the role of intracellular Ca^{2+}, we treated the cells with 1,2-bis(2-aminophenoxy)ethane-*N*,*N*,*N*′,*N*′-tetraacetic acid tetrakis-acetoxymethyl ester to chelate intracellular calcium and found that isoproterenol no longer modulated cell deformability (Fig. 1*H*). Taken together, these results support that activation of β-AR signaling pathway modulates macrophage deformability.

F-actin mediates β-AR–induced changes in cell deformability

The actin cytoskeleton is a major determinant of cell deformability (43, 44). Specifically, levels of filamentous (F)-actin are critical for regulating cellular shape and mechanotype (45, 46). To investigate whether the effect of β-AR signaling on macrophage deformability was linked to changes in the actin cytoskeleton, we imaged F-actin using phalloidin staining and confocal microscopy. Quantitative image analysis revealed that treatment with isoproterenol for 24 h increased phalloidin intensity by 1.4-fold—indicating increased F-actin density ($P < 0.001$) (**Fig. 2*A*, *B***). We observed that the increase in F-actin intensity occurred in the cytoplasm, but not in the nuclear region (P = 0.11; Fig. 2*A*–*C*). These analyses investigated actin distribution across a 2 μm-thick midplane section of individual cells, and future studies that image actin through the axial dimension of cells will be important to identify spatial differences in actin throughout the cell body. Nonetheless, consistent with these initial findings, we reported previously that β-AR signaling increases F-actin in tumor cells on similar timescales (32).

To further explore the role of the actin cytoskeleton in β-AR regulation of macrophage deformability, we next examined the role of different actin filament populations.

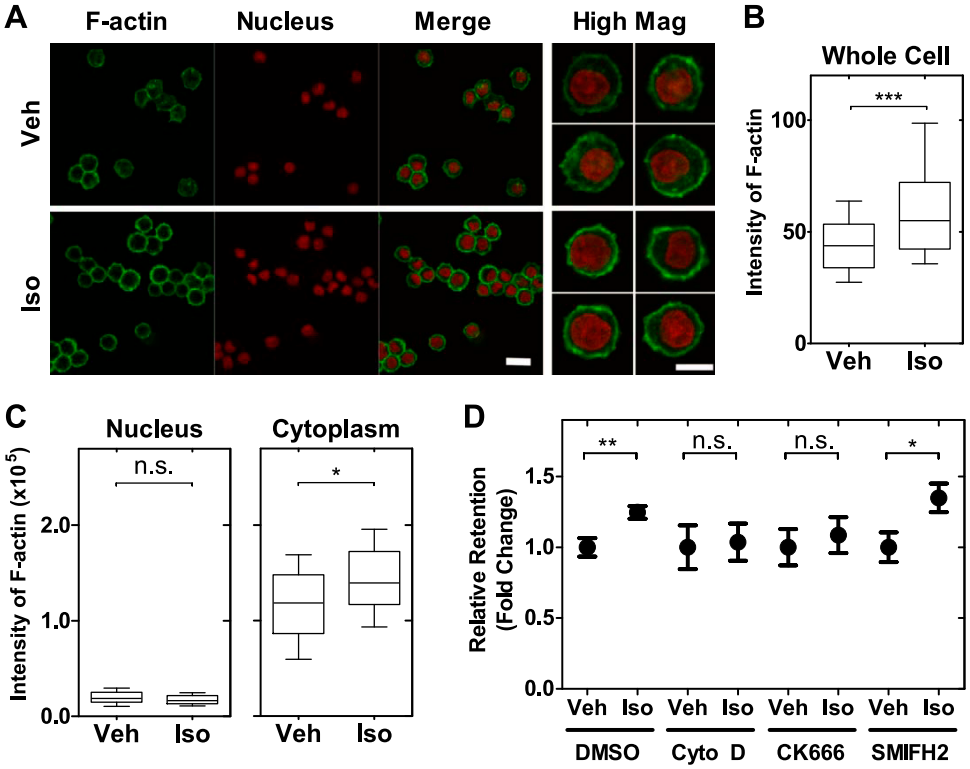

Figure 2. Actin contributes to changes in cell mechanotype induced by β-AR. *A*) Representative images of macrophages treated with either vehicle or isoproterenol for 24 h followed by staining to visualize F-actin (phalloidin) and nucleus (DRAQ5). Scale bar, 20 μm. High Mag (Original magnification, ×63): representative images are confocal sections acquired at the midplane of individual cells with a slice thickness of 2 μm. Scale bar, 10 μm. *B*) Quantitative analysis of F-actin intensity in vehicle or isoproterenol-treated cells ($n > 1000$). Boxplot shows the lower and upper quartiles with median (line). Whiskers show the 10–90th percentiles. Unpaired t test. ***$P < 0.001$. *C*) Quantitative analysis of F-actin intensity in nuclear and cytoplasmic regions from high mag images (n = 30). Boxplot shows the lower and upper quartiles with median (line). Whiskers show the 10–90th percentiles. Unpaired t test. *$P < 0.05$. *D*) Macrophage retention measured by PMF. Cells are treated with inhibitors of F-actin polymerization [cytochalasin D (Cyto D) 2 μM for 1 h], Arp2/3 activity (CK666, 50 μM for 24 h), or formin activity (SMIFH2, 20 μM for 24 h). One-way ANOVA test with Tukey's multiple comparison test. *$P < 0.05$, **$P < 0.01$. N.s., not significant. Results represent data from at least 3 independent experiments (N = 3).

There are 2 major actin filament populations that are nucleated by formins and the Arp2/3 complex. Formins nucleate linear actin filaments and promote elongation, resulting in long, linear filaments (47, 48). The Arp2/3 complex also nucleates actin filaments, but generates branched F-actin filament networks that tend to be ~10× shorter and have ~20× faster turnover than formin-nucleated filaments (44, 49, 50). We found that treatment with the Arp2/3 inhibitor, CK666, or inhibitor of actin polymerization, cytochalasin D, blocked the ability of isoproterenol to increase macrophage retention, indicating that β-AR regulation of deformability is dependent on actin polymerization and branching. By contrast, treatment with the formin-inhibitor SMIFH2 did not reverse the effect of isoproterenol on retention ($P = 0.02$), indicating that formins are not a major determinant of β-AR regulation of macrophage deformability (Fig. 2*D*). These findings suggest that the effects of β-AR activation on macrophage deformability are predominantly mediated by Arp2/3-associated shorter, branched filament networks rather than unbranched filaments.

Activation of β-AR signaling increases macrophage phagocytosis and migration

Macrophages respond to chemotactic cues within tissues and move to the site of infection to eliminate pathogens by phagocytosis. To investigate whether β-AR signaling modulates these key macrophage functions, we treated macrophages with isoproterenol and measured phagocytosis and migration. Isoproterenol treatment increased phagocytosis of fluorescent *E.coli* bioparticles by 44% compared with vehicle-treated cells ($P < 0.001$) (**Fig. 3*A, B*** and Supplemental Fig. S1*I*). Pretreatment with the β-AR antagonist propranolol blocked isoproterenol-enhanced *E.coli* internalization, showing the effect of isoproterenol on phagocytosis is dependent on the β-AR. In contrast, forskolin treatment enhanced phagocytosis, demonstrating a role for cAMP in regulating phagocytosis (Fig. 3*A, B*); these findings are consistent with modulation of phagocytosis by the β-AR signaling pathway.

To investigate the effect of β-AR activation on migration, we used a transwell migration assay to quantify migration of macrophages through 5 μm pores toward a serum gradient. We found that isoproterenol increased the number of cells that migrated through the porous membrane toward a serum gradient by 2.4-fold ($P < 0.001$), reflecting that β-AR activation enhances macrophage migration (Fig. 3*C, D*). Enhanced migration was also observed with forskolin treatment, but blocked by propranolol (Fig. 3*C, D*); these findings are consistent with regulation through the β-AR signaling pathway.

Because actin remodeling is critical for the β-AR–induced change in cell deformability, we next asked whether changes in actin filament organization also contribute to the β-AR-mediated increase in macrophage phagocytosis and migration. To determine the effects of changes in actin organization on phagocytosis and migration, we treated macrophages with inhibitors to block actin nucleation, polymerization, and branching. We found that inhibiting actin polymerization (Cyto D) or

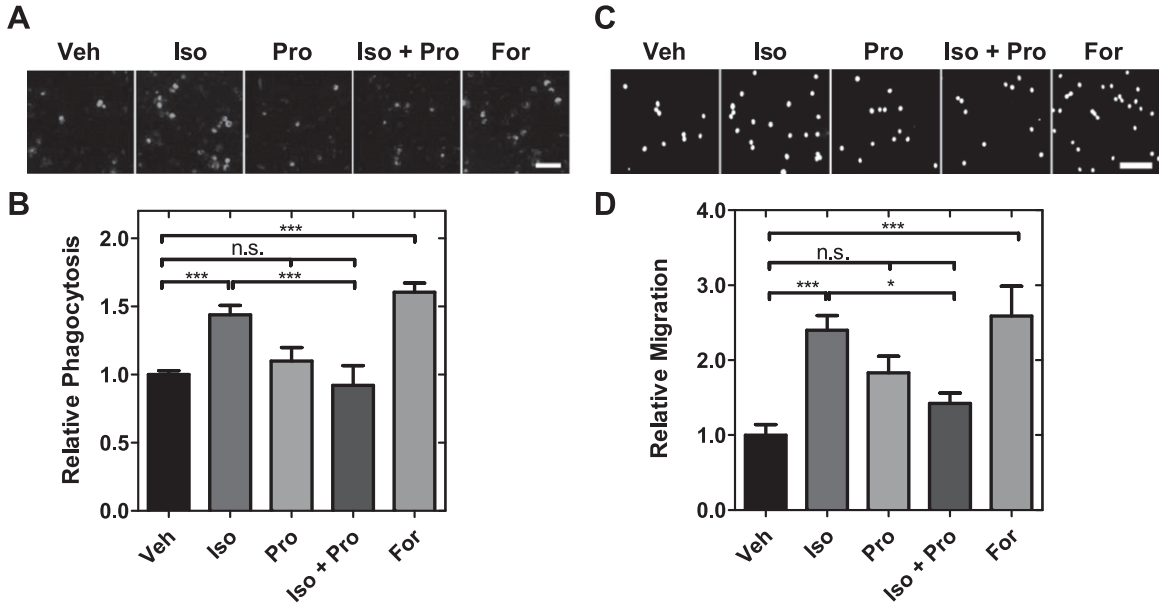

Figure 3. β-AR activation increases phagocytosis and motility in macrophages. *A*) Representative images from phagocytosis assay showing cells treated with vehicle control (Veh), isoproterenol (Iso), propranolol (Pro), or forskolin (For) for 25 h. Green signal shows internalized *E.coli* bioparticles after drug treatments. Scale bar, 50 μm. *B*) Relative phagocytosis shows number of internalized beads relative to vehicle control. Bars show means ± SE. One-way ANOVA test with Tukey's multiple comparison test. ***$P < 0.001$. *C*) Representative images from transwell migration assay. Scale bar, 100 μm. *D*) Number of migrated cells is determined by counting the number of nuclei in bottom chamber. One-way ANOVA test with Tukey's multiple comparison test. *$P < 0.05$, ***$P < 0.001$. N.s., not significant. Results represent data from at least 3 independent experiments ($N = 3$).

nucleation of unbranched filaments (SMIFH2) reduced basal levels of phagocytosis (**Fig. 4*A***) and migration (Fig. 4*B*) and prevented isoproterenol from increasing either phagocytosis or migration. Interestingly, we observed the Arp2/3 inhibitor CK666 had no significant effects on basal levels of phagocytosis and migration, but blocked the β-AR–induced increase in phagocytosis and migration (Fig. 4).

Taken together our findings show that β-AR modulation of actin organization and dynamics regulates phagocytosis and migration (**Fig. 5**), which are required for immune response. Our results also suggest that β-AR signaling regulates macrophage deformability by shifting the balance between longer, linear branched filaments of the actin cytoskeleton in favor of a highly dynamic network that exhibits more branching and shorter filaments (Fig. 5).

DISCUSSION

We show here that β-AR signaling triggers changes in cell mechanotype, phagocytosis, and migration that are mediated by changes in the organization of actin (Fig. 5). Although there is evidence that cell mechanical properties are linked with immune cell functions (16, 17, 51), mechanistic knowledge of how physiologic cues elicit such physical changes is still developing. Our results discriminate between the roles of formin-nucleated and Arp2/3-nucleated actin filaments in stress hormone regulation of macrophage deformability: our findings suggest that β-AR activation shifts the balance between actin filament populations to favor more highly branched, Arp2/3-mediated structures rather than linear unbranched filaments (Fig. 5). These results align well with recent observations of actin organization at adherens junctions, where bundles of nonmuscle myosin II-associated linear actin filaments run parallel to the plasma membrane and Arp2/3-associated branched networks emanate from these bundles and appear to push against the membrane (52). Our findings suggest that a similar organization may exist in macrophages where bundles of linear actin filaments provide basal stiffness; consistent with this, previous studies show that linear actin filaments are a major determinant of cell stiffness (44). Here, we show that the shift toward branched actin networks induced by β-AR activation is a major contributor to the observed decrease in cellular deformability. Given that Arp-2/3-nucleated filaments have ~20× faster turnover than formin-nucleated filaments (44), it is intriguing to speculate that the shift to the more highly dynamic, Arp2/3-nucleated actin structures with stress hormone stimulation may enable cells to more quickly sample their environment and respond appropriately to external stimuli.

The finding that β-AR regulation of macrophage deformability depends on Arp2/3 suggests that both the organization and dynamics of actin may be important for regulation of cell mechanotype by soluble stress hormones. Branched actin structures proximal to the plasma membrane (52) counter the contractile forces generated by nonmuscle myosin II to increase cortical tension and cell stiffness (53, 54). Kinetic processes of actin nucleation and branching also contribute to cellular stiffness and force generation (44, 53, 55), which enable cells to effectively generate protrusive structures—such as lamellipodia and podosomes—to enhance key functions of phagocytosis and motility (22, 23, 56–59).

By demonstrating a key role for actin in β-AR regulation of phagocytosis and motility, the findings presented here provide mechanistic insight into previous studies that found increased phagocytosis of primary macrophages with β-AR activation (13) as well as observations that macrophage deformability is associated with phagocytosis (19, 59). Our results show that inhibition of Arp2/3 or formin activity blocks the β-AR–induced increase in phagocytosis, consistent with the role of actin polymerization and branching in generating protrusions required to engulf particles (60–62). The activity of Arp2/3 and formins is also critical for the motility of macrophages and dendritic cells (63–65), where force generation is required for the formation of protrusive structures that promote

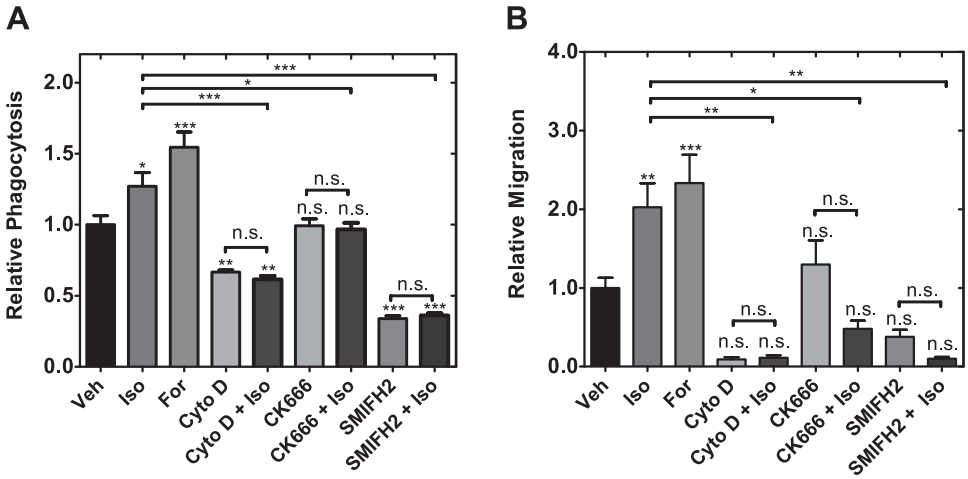

Figure 4. β-AR signaling regulates macrophage functions through changes in actin organization. *A*) Phagocytosis is measured in the presence of actin polymerization inhibitor (2 μM cytochalasin D), Arp2/3 inhibitor (50 μM CK666), or formin inhibitor (20 μM SMIFH2), whereas β-AR signaling is activated with 100 nM isoproterenol for 24 h. Statistical significance indicated by asterisks shows comparisons to vehicle control unless indicated. One-way ANOVA test with Tukey's multiple comparison test. $^*P < 0.05$, $^{**}P < 0.01$, $^{***}P < 0.001$. *B*) Quantitative analysis of chemotaxis after 24 h of drug treatment. Statistical significance indicated by asterisks shows comparisons to vehicle control unless indicated. One-way ANOVA test with Tukey's multiple comparison test. $^*P < 0.05$, $^{**}P < 0.01$, $^{***}P < 0.001$. N.s., not significant. Results represent data from at least 3 independent experiments ($N = 3$).

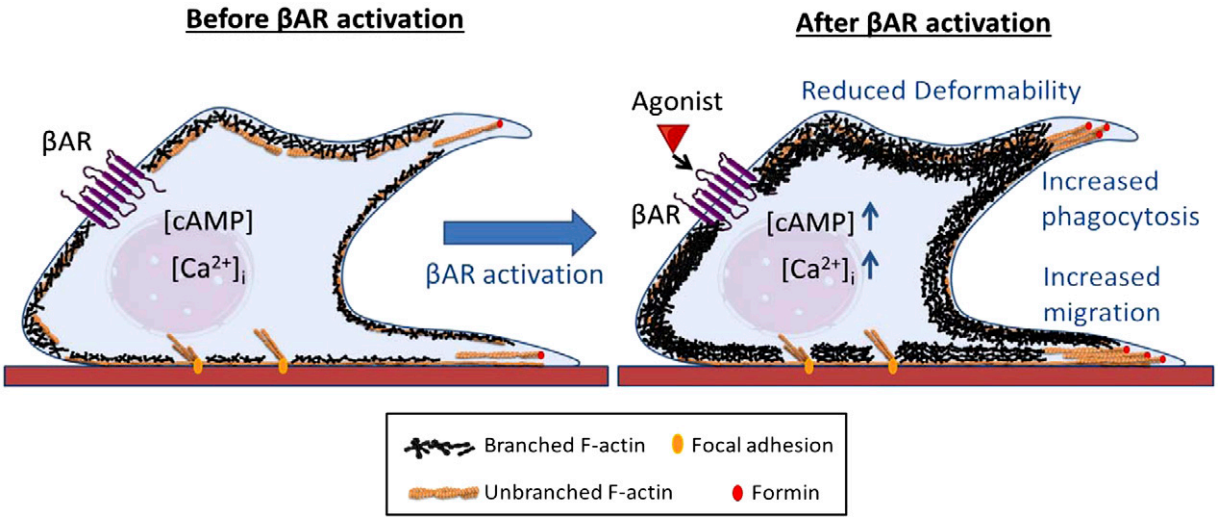

Figure 5. Proposed mechanism for β-AR regulation of macrophage deformability and function. Activation of β-AR signaling with agonist results in reduced whole cell deformability and increased branched, Arp2/3-nucleated actin in the cytoplasm. β-AR activation also enhances macrophage functions such as phagocytosis and migration.

invasion (66, 67). Arp2/3 was also recently identified to contribute to the deformation of the nucleus during the migration of cells through narrow gaps (64). It is plausible that β-AR activation may enhance the ability of cells to move through micron-scale pores *via* increased nuclear translocation mediated by Arp2/3-generated forces. Cell motility is also sensitive to myosin II activity (68), and our previous findings in cancer cells showed that a β_2AR–actin-myosin II axis mediates cell stiffness and motility (32). Future studies will investigate how β-AR signaling regulates the interplay between branched, Arp2/3-nucleated actin and myosin II, which is associated primarily with linear, formin-nucleated filaments (69, 70).

Although associations between cell mechanotype and function have been observed in other immune cell contexts, the molecular mechanisms have not been well understood. The ability of neutrophils to deform through narrow gaps is critical for their chemotactic functions. Indeed, neutrophils show increased compliance and faster advection through 12 μm narrow microfluidic channels; by contrast, macrophages exhibit reduced steady-state viscosity compared with neutrophils, which may be a physiologic adaptation for enhanced migration through tissues (18). The mechanotype of T cells influences the size of immune synapses formed with antigen presenting cells (APCs) and thus plays a crucial role in their signaling and activation: the more compliant cytoskeleton of active T cells compared with naïve T cells results in formation of larger immune synapses with APCs, because a more compliant T cell can more readily deform around or "hug" the APC (71). These findings suggest that cellular deformability serves as an important characteristic in predicting T cell interactions with APCs and their subsequent activation. Consistent with our findings that actin organization and dynamics link macrophage mechanotype and function, the actin-severing factor cofilin was found to be critical for modulating T cell deformability and immune synapses with APCs (71). Actin remodeling is also critical for intracellular trafficking and receptor internalization and sensitization (72–74); in future research it will be important to determine how these cellular functions are regulated by signaling through β-AR. Further studies of the biophysical and molecular mechanisms of immune cell functions will provide a more detailed understanding of the range of soluble and mechanical cues that regulate immune cell behaviors. For example, matrix stiffness regulates immune cell mechanotype (75, 76), cytokine production (77–79), and phagocytosis (19) and also determines migration mode (80, 81). Understanding how multiple soluble and mechanical cues in the microenvironment contribute to immune cell behaviors will be important to define immune response in physiologic and disease contexts. FJ

ACKNOWLEDGMENTS

The authors thank Dr. Sherie L. Morrison [University of California, Los Angeles (UCLA)] for providing U937 cell line, and the UCLA Statistical Consulting Group for advice on data analysis. Flow cytometry ImageStream, and IncuCyte analyses were performed in the UCLA Flow Cytometry Core Facility, which is supported by U.S. National Institutes of Health (NIH) Awards CA-16042 (National Cancer Institute) and AI-28697 (National Institute of Allergy and Infectious Diseases) and by the Jonsson Comprehensive Cancer Center, the Center for AIDS Research, and the David Geffen School of Medicine at UCLA. This work was supported by NIH/National Center for Advancing Translational Science (NCATS) UCLA Clinical and Translational Science Institute Grant UL1TR000124, the University of California Cancer Research Coordinating Committe (CRR-18-52690), the National Science Foundation (CAREER DBI-1254185 to A.C.R.), and the Australian National Health and Medical Research Council (NHMRC) APP1147498. The authors declare no conflicts of interest.

AUTHOR CONTRIBUTIONS

T.-H. Kim, E. K. Sloan, and A. C. Rowat designed the experiments; T.-H. Kim, C. Ly, and A. Christodoulides performed experiments; T.-H. Kim, C. Ly, C. J. Nowell, P. W. Gunning, E. K. Sloan, and A. C. Rowat analyzed and

interpreted data; and T.-H. Kim, P. W. Gunning, E. K. Sloan, and A. C. Rowat wrote the manuscript.

REFERENCES

1. Okabe, Y., and Medzhitov, R. (2014) Tissue-specific signals control reversible program of localization and functional polarization of macrophages. *Cell* **157**, 832–844
2. Nguyen, K. D., Qiu, Y., Cui, X., Goh, Y. P. S., Mwangi, J., David, T., Mukundan, L., Brombacher, F., Locksley, R. M., and Chawla, A. (2011) Alternatively activated macrophages produce catecholamines to sustain adaptive thermogenesis. *Nature* **480**, 104–108
3. Lavin, Y., Winter, D., Blecher-Gonen, R., David, E., Keren-Shaul, H., Merad, M., Jung, S., and Amit, I. (2014) Tissue-resident macrophage enhancer landscapes are shaped by the local microenvironment. *Cell* **159**, 1312–1326
4. Nicholls, A. J., Wen, S. W., Hall, P., Hickey, M. J., and Wong, C. H. Y. (2018) Activation of the sympathetic nervous system modulates neutrophil function. *J. Leukoc. Biol.* **103**, 295–309
5. Wirth, T., Westendorf, A. M., Bloemker, D., Wildmann, J., Engler, H., Mollerus, S., Wadwa, M., Schäfer, M. K.-H., Schedlowski, M., and del Rey, A. (2014) The sympathetic nervous system modulates CD4(+)Foxp3(+) regulatory T cells via noradrenaline-dependent apoptosis in a murine model of lymphoproliferative disease. *Brain Behav. Immun.* **38**, 100–110
6. Cao, X., and Aballay, A. (2016) Neural inhibition of dopaminergic signaling enhances immunity in a cell-non-autonomous manner. *Curr. Biol.* **26**, 2398
7. Dantzer, R. (2018) Neuroimmune interactions: from the brain to the immune system and vice versa. *Physiol. Rev.* **98**, 477–504
8. Epelman, S., Lavine, K. J., and Randolph, G. J. (2014) Origin and functions of tissue macrophages. *Immunity* **41**, 21–35
9. Shapouri-Moghaddam, A., Mohammadian, S., Vazini, H., Taghadosi, M., Esmaeili, S.-A., Mardani, F., Seifi, B., Mohammadi, A., Afshari, J. T., and Sahebkar, A. (2018) Macrophage plasticity, polarization, and function in health and disease. *J. Cell. Physiol.* **233**, 6425–6440
10. Honold, L., and Nahrendorf, M. (2018) Resident and monocyte-derived macrophages in cardiovascular disease. *Circ. Res.* **122**, 113–127
11. Chen, Y., and Zhang, X. (2017) Pivotal regulators of tissue homeostasis and cancer: macrophages. *Exp. Hematol. Oncol.* **6**, 23
12. Chiarella, S. E., Soberanes, S., Urich, D., Morales-Nebreda, L., Nigdelioglu, R., Green, D., Young, J. B., Gonzalez, A., Rosario, C., Misharin, A. V., Ghio, A. J., Wunderink, R. G., Donnelly, H. K., Radigan, K. A., Perlman, H., Chandel, N. S., Budinger, G. R. S., and Mutlu, G. M. (2014) β_2-Adrenergic agonists augment air pollution-induced IL-6 release and thrombosis. *J. Clin. Invest.* **124**, 2935–2946
13. Muthu, K., He, L.-K., Szilagyi, A., Strotmon, P., Gamelli, R. L., and Shankar, R. (2010) ß-adrenergic stimulation increases macrophage CD14 expression and E. coli phagocytosis through PKA signaling mechanisms. *J. Leukoc. Biol.* **88**, 715–724
14. Izeboud, C. A., Mocking, J. A., Monshouwer, M., van Miert, A. S., and Witkamp, R. F. (1999) Participation of beta-adrenergic receptors on macrophages in modulation of LPS-induced cytokine release. *J. Recept. Signal Transduct. Res.* **19**, 191–202
15. Serio, M., Potenza, M. A., Montagnani, M., Mansi, G., Mitolo-Chieppa, D., and Jirillo, E. (1996) Beta-adrenoceptor responsiveness of splenic macrophages in normotensive and hypertensive rats. *Immunopharmacol. Immunotoxicol.* **18**, 247–265
16. Lam, J., Herant, M., Dembo, M., and Heinrich, V. (2009) Baseline mechanical characterization of J774 macrophages. *Biophys. J.* **96**, 248–254
17. Ekpenyong, A. E., Toepfner, N., Fiddler, C., Herbig, M., Li, W., Cojoc, G., Summers, C., Guck, J., and Chilvers, E. R. (2017) Mechanical deformation induces depolarization of neutrophils. *Sci. Adv.* **3**, e1602536
18. Ekpenyong, A. E., Whyte, G., Chalut, K., Pagliara, S., Lautenschläger, F., Fiddler, C., Paschke, S., Keyser, U. F., Chilvers, E. R., and Guck, J. (2012) Viscoelastic properties of differentiating blood cells are fate- and function-dependent. *PLoS One* **7**, e45237
19. Patel, N. R., Bole, M., Chen, C., Hardin, C. C., Kho, A. T., Mih, J., Deng, L., Butler, J., Tschumperlin, D., Fredberg, J. J., Krishnan, R., and Koziel, H. (2012) Cell elasticity determines macrophage function. *PLoS One* **7**, e41024
20. Bufi, N., Saitakis, M., Dogniaux, S., Buschinger, O., Bohineust, A., Richert, A., Maurin, M., Hivroz, C., and Asnacios, A. (2015) Human primary immune cells exhibit distinct mechanical properties that are modified by inflammation. *Biophys. J.* **108**, 2181–2190
21. Rougerie, P., Miskolci, V., and Cox, D. (2013) Generation of membrane structures during phagocytosis and chemotaxis of macrophages: role and regulation of the actin cytoskeleton. *Immunol. Rev.* **256**, 222–239
22. Kage, F., Winterhoff, M., Dimchev, V., Mueller, J., Thalheim, T., Freise, A., Brühmann, S., Kollasser, J., Block, J., Dimchev, G., Geyer, M., Schnittler, H.-J., Brakebusch, C., Stradal, T. E. B., Carlier, M.-F., Sixt, M., Käs, J., Faix, J., and Rottner, K. (2017) FMNL formins boost lamellipodial force generation. *Nat. Commun.* **8**, 14832
23. Labernadie, A., Bouissou, A., Delobelle, P., Balor, S., Voituriez, R., Proag, A., Fourquaux, I., Thibault, C., Vieu, C., Poincloux, R., Charrière, G. M., and Maridonneau-Parini, I. (2014) Protrusion force microscopy reveals oscillatory force generation and mechanosensing activity of human macrophage podosomes. *Nat. Commun.* **5**, 5343
24. Chitu, V., Pixley, F. J., Macaluso, F., Larson, D. R., Condeelis, J., Yeung, Y.-G., and Stanley, E. R. (2005) The PCH family member MAYP/PSTPIP2 directly regulates F-actin bundling and enhances filopodia formation and motility in macrophages. *Mol. Biol. Cell* **16**, 2947–2959
25. Hida, A., Kawakami, A., Nakashima, T., Yamasaki, S., Sakai, H., Urayama, S., Ida, H., Nakamura, H., Migita, K., Kawabe, Y., and Eguchi, K. (2000) Nuclear factor-kappaB and caspases co-operatively regulate the activation and apoptosis of human macrophages. *Immunology* **99**, 553–560
26. Wan, C. P., Park, C. S., and Lau, B. H. (1993) A rapid and simple microfluorometric phagocytosis assay. *J. Immunol. Methods* **162**, 1–7
27. Kapellos, T. S., Taylor, L., Lee, H., Cowley, S. A., James, W. S., Iqbal, A. J., and Greaves, D. R. (2016) A novel real time imaging platform to quantify macrophage phagocytosis. *Biochem. Pharmacol.* **116**, 107–119
28. Schindelin, J., Arganda-Carreras, I., Frise, E., Kaynig, V., Longair, M., Pietzsch, T., Preibisch, S., Rueden, C., Saalfeld, S., Schmid, B., Tinevez, J.-Y., White, D. J., Hartenstein, V., Eliceiri, K., Tomancak, P., and Cardona, A. (2012) Fiji: an open-source platform for biological-image analysis. *Nat. Methods* **9**, 676–682
29. Qi, D., Kaur Gill, N., Santiskulvong, C., Sifuentes, J., Dorigo, O., Rao, J., Taylor-Harding, B., Ruprecht Wiedemeyer, W., and Rowat, A. C. (2015) Screening cell mechanotype by parallel microfiltration. *Sci. Rep.* **5**, 17595
30. Gill, N. K., Gill, N. K., Qi, D., Kim, T.-H., Chan, C., Nguyen, A., Nyberg, K. D., and Rowat, A. C. (2017) A protocol for screening cells based on deformability using parallel microfiltration. *Protoc. Exch.* doi: 10.1038/protex.2017.101
31. Nyberg, K. D., Hu, K. H., Kleinman, S. H., Khismatullin, D. B., Butte, M. J., and Rowat, A. C. (2017) Quantitative deformability cytometry: rapid, calibrated measurements of cell mechanical properties. *Biophys. J.* **113**, 1574–1584
32. Kim, T.-H., Gill, N. K., Nyberg, K. D., Nguyen, A. V., Hohlbauch, S. V., Geisse, N. A., Nowell, C. J., Sloan, E. K., and Rowat, A. C. (2016) Cancer cells become less deformable and more invasive with activation of β-adrenergic signaling. *J. Cell Sci.* **129**, 4563–4575
33. Nyberg, K. D., Scott, M. B., Bruce, S. L., Gopinath, A. B., Bikos, D., Mason, T. G., Kim, J. W., Choi, H. S., and Rowat, A. C. (2016) The physical origins of transit time measurements for rapid, single cell mechanotyping. *Lab Chip* **16**, 3330–3339
34. Hoelzle, D. J., Varghese, B. A., Chan, C. K., and Rowat, A. C. (2014) A microfluidic technique to probe cell deformability. *J. Vis. Exp.* **91**, e51474
35. Liu, M. Y., and Wu, M. C. (1992) Induction of human monocyte cell line U937 differentiation and CSF-1 production by phorbol ester. *Exp. Hematol.* **20**, 974–979
36. Yang, L., Dai, F., Tang, L., Le, Y., and Yao, W. (2017) Macrophage differentiation induced by PMA is mediated by activation of RhoA/ROCK signaling. *J. Toxicol. Sci.* **42**, 763–771
37. Groot-Kormelink, P. J., Fawcett, L., Wright, P. D., Gosling, M., and Kent, T. C. (2012) Quantitative GPCR and ion channel transcriptomics in primary alveolar macrophages and macrophage surrogates. *BMC Immunol.* **13**, 57
38. Verhoeckx, K. C. M., Bijlsma, S., de Groene, E. M., Witkamp, R. F., van der Greef, J., and Rodenburg, R. J. T. (2004) A combination of proteomics, principal component analysis and transcriptomics is a powerful tool for the identification of biomarkers for macrophage maturation in the U937 cell line. *Proteomics* **4**, 1014–1028
39. Harris, P., and Ralph, P. (1985) Human leukemic models of myelomonocytic development: a review of the HL-60 and U937 cell lines. *J. Leukoc. Biol.* **37**, 407–422

40. Creed, S. J., Le, C. P., Hassan, M., Pon, C. K., Albold, S., Chan, K. T., Berginski, M. E., Huang, Z., Bear, J. E., Lane, J. R., Halls, M. L., Ferrari, D., Nowell, C. J., and Sloan, E. K. (2015) β2-adrenoceptor signaling regulates invadopodia formation to enhance tumor cell invasion. *Breast Cancer Res.* **17**, 145
41. Pon, C. K., Lane, J. R., Sloan, E. K., and Halls, M. L. (2016) The β2-adrenoceptor activates a positive cAMP-calcium feedforward loop to drive breast cancer cell invasion. *FASEB J.* **30**, 1144–1154
42. Qin, J. F., Jin, F. J., Li, N., Guan, H. T., Lan, L., Ni, H., and Wang, Y. (2015) Adrenergic receptor β2 activation by stress promotes breast cancer progression through macrophages M2 polarization in tumor microenvironment. *BMB Rep.* **48**, 295–300
43. MacQueen, L. A., Thibault, M., Buschmann, M. D., and Wertheimer, M. R. (2012) Electromechanical deformation of mammalian cells in suspension depends on their cortical actin thicknesses. *J. Biomech.* **45**, 2797–2803
44. Fritzsche, M., Erlenkämper, C., Moeendarbary, E., Charras, G., and Kruse, K. (2016) Actin kinetics shapes cortical network structure and mechanics. *Sci. Adv.* **2**, e1501337
45. Prentki, M., Chaponnier, C., Jeanrenaud, B., and Gabbiani, G. (1979) Actin microfilaments, cell shape, and secretory processes in isolated rat hepatocytes. Effect of phalloidin and cytochalasin D. *J. Cell Biol.* **81**, 592–607
46. Tsai, M. A., Frank, R. S., and Waugh, R. E. (1994) Passive mechanical behavior of human neutrophils: effect of cytochalasin B. *Biophys. J.* **66**, 2166–2172
47. Schönichen, A., and Geyer, M. (2010) Fifteen formins for an actin filament: a molecular view on the regulation of human formins. *Biochim. Biophys. Acta* **1803**, 152–163
48. Chesarone, M. A., and Goode, B. L. (2009) Actin nucleation and elongation factors: mechanisms and interplay. *Curr. Opin. Cell Biol.* **21**, 28–37
49. Pizarro-Cerdá, J., Chorev, D. S., Geiger, B., and Cossart, P. (2017) The diverse family of arp2/3 complexes. *Trends Cell Biol.* **27**, 93–100
50. Pollard, T. D., and Beltzner, C. C. (2002) Structure and function of the Arp2/3 complex. *Curr. Opin. Struct. Biol.* **12**, 768–774
51. Di Cerbo, A., Rubino, V., Morelli, F., Ruggiero, G., Landi, R., Guidetti, G., Canello, S., Terrazzano, G., and Alessandrini, A. (2018) Mechanical phenotyping of K562 cells by the micropipette aspiration technique allows identifying mechanical changes induced by drugs. *Sci. Rep.* **8**, 1219
52. Efimova, N., and Svitkina, T. M. (2018) Branched actin networks push against each other at adherens junctions to maintain cell-cell adhesion. *J. Cell Biol.* **217**, 1827–1845
53. Fletcher, D. A., and Mullins, R. D. (2010) Cell mechanics and the cytoskeleton. *Nature* **463**, 485–492
54. Gabriele, S., Benoliel, A.-M., Bongrand, P., and Théodoly, O. (2009) Microfluidic investigation reveals distinct roles for actin cytoskeleton and myosin II activity in capillary leukocyte trafficking. *Biophys. J.* **96**, 4308–4318
55. Cojoc, D., Difato, F., Ferrari, E., Shahapure, R. B., Laishram, J., Righi, M., Di Fabrizio, E. M., and Torre, V. (2007) Properties of the force exerted by filopodia and lamellipodia and the involvement of cytoskeletal components. *PLoS One* **2**, e1072
56. Dimchev, G., Steffen, A., Kage, F., Dimchev, V., Pernier, J., Carlier, M.-F., and Rottner, K. (2017) Efficiency of lamellipodia protrusion is determined by the extent of cytosolic actin assembly. *Mol. Biol. Cell* **28**, 1311–1325
57. Isogai, T., van der Kammen, R., Leyton-Puig, D., Kedziora, K. M., Jalink, K., and Innocenti, M. (2015) Initiation of lamellipodia and ruffles involves cooperation between mDia1 and the Arp2/3 complex. *J. Cell Sci.* **128**, 3796–3810
58. Revach, O.-Y., Weiner, A., Rechav, K., Sabanay, I., Livne, A., and Geiger, B. (2015) Mechanical interplay between invadopodia and the nucleus in cultured cancer cells. *Sci. Rep.* **5**, 9466
59. Mazur, M. T., and Williamson, J. R. (1977) Macrophage deformability and phagocytosis. *J. Cell Biol.* **75**, 185–199
60. Hoffmann, A.-K., Naj, X., and Linder, S. (2014) Daam1 is a regulator of filopodia formation and phagocytic uptake of Borrelia burgdorferi by primary human macrophages. *FASEB J.* **28**, 3075–3089
61. May, R. C., Caron, E., Hall, A., and Machesky, L. M. (2000) Involvement of the Arp2/3 complex in phagocytosis mediated by FcgammaR or CR3. *Nat. Cell Biol.* **2**, 246–248
62. May, R. C., and Machesky, L. M. (2001) Phagocytosis and the actin cytoskeleton. *J. Cell Sci.* **114**, 1061–1077
63. Bendell, A. C., Williamson, E. K., Chen, C. S., Burkhardt, J. K., and Hammer, D. A. (2017) The Arp2/3 complex binding protein HS1 is required for efficient dendritic cell random migration and force generation. *Integr. Biol.* **9**, 695–708
64. Thiam, H.-R., Vargas, P., Carpi, N., Crespo, C. L., Raab, M., Terriac, E., King, M. C., Jacobelli, J., Alberts, A. S., Stradal, T., Lennon-Dumenil, A.-M., and Piel, M. (2016) Perinuclear Arp2/3-driven actin polymerization enables nuclear deformation to facilitate cell migration through complex environments. *Nat. Commun.* **7**, 10997
65. Miller, M. R., Miller, E. W., and Blystone, S. D. (2017) Non-canonical activity of the podosomal formin FMNL1γ supports immune cell migration. *J. Cell Sci.* **130**, 1730–1739
66. Jevnikar, Z., Mirković, B., Fonović, U. P., Zidar, N., Švajger, U., and Kos, J. (2012) Three-dimensional invasion of macrophages is mediated by cysteine cathepsins in protrusive podosomes. *Eur. J. Immunol.* **42**, 3429–3441
67. Li, A., Dawson, J. C., Forero-Vargas, M., Spence, H. J., Yu, X., König, I., Anderson, K., and Machesky, L. M. (2010) The actin-bundling protein fascin stabilizes actin in invadopodia and potentiates protrusive invasion. *Curr. Biol.* **20**, 339–345
68. Vicente-Manzanares, M., Ma, X., Adelstein, R. S., and Horwitz, A. R. (2009) Non-muscle myosin II takes centre stage in cell adhesion and migration. *Nat. Rev. Mol. Cell Biol.* **10**, 778–790
69. Van den Dries, K., Meddens, M. B. M., de Keijzer, S., Shekhar, S., Subramaniam, V., Figdor, C. G., and Cambi, A. (2013) Interplay between myosin IIA-mediated contractility and actin network integrity orchestrates podosome composition and oscillations. *Nat. Commun.* **4**, 1412
70. Rottner, K., Faix, J., Bogdan, S., Linder, S., and Kerkhoff, E. (2017) Actin assembly mechanisms at a glance. *J. Cell Sci.* **130**, 3427–3435
71. Thauland, T. J., Hu, K. H., Bruce, M. A., and Butte, M. J. (2017) Cytoskeletal adaptivity regulates T cell receptor signaling. *Sci. Signal.* **10**, eaah3737
72. Zhang, Y., Shen, H., Liu, H., Feng, H., Liu, Y., Zhu, X., and Liu, X. (2017) Arp2/3 complex controls T cell homeostasis by maintaining surface TCR levels via regulating TCR^+ endosome trafficking. *Sci. Rep.* **7**, 8952
73. Wheeler, D., Sneddon, W. B., Wang, B., Friedman, P. A., and Romero, G. (2007) NHERF-1 and the cytoskeleton regulate the traffic and membrane dynamics of G protein-coupled receptors. *J. Biol. Chem.* **282**, 25076–25087
74. Itagaki, K., Kannan, K. B., Singh, B. B., and Hauser, C. J. (2004) Cytoskeletal reorganization internalizes multiple transient receptor potential channels and blocks calcium entry into human neutrophils. *J. Immunol.* **172**, 601–607
75. Oakes, P. W., Patel, D. C., Morin, N. A., Zitterbart, D. P., Fabry, B., Reichner, J. S., and Tang, J. X. (2009) Neutrophil morphology and migration are affected by substrate elasticity. *Blood* **114**, 1387–1395
76. Mennens, S. F. B., Bolomini-Vittori, M., Weiden, J., Joosten, B., Cambi, A., and van den Dries, K. (2017) Substrate stiffness influences phenotype and function of human antigen-presenting dendritic cells. *Sci. Rep.* **7**, 17511
77. Previtera, M. L., and Sengupta, A. (2015) Substrate stiffness regulates proinflammatory mediator production through TLR4 activity in macrophages. *PLoS One* **10**, e0145813
78. McWhorter, F. Y., Davis, C. T., and Liu, W. F. (2015) Physical and mechanical regulation of macrophage phenotype and function. *Cell. Mol. Life Sci.* **72**, 1303–1316
79. Blakney, A. K., Swartzlander, M. D., and Bryant, S. J. (2012) The effects of substrate stiffness on the in vitro activation of macrophages and in vivo host response to poly(ethylene glycol)-based hydrogels. *J. Biomed. Mater. Res. A.* **100**, 1375–1386
80. Van Goethem, E., Poincloux, R., Gauffre, F., Maridonneau-Parini, I., and Le Cabec, V. (2010) Matrix architecture dictates three-dimensional migration modes of human macrophages: differential involvement of proteases and podosome-like structures. *J. Immunol.* **184**, 1049–1061
81. Salmon, H., Franciszkiewicz, K., Damotte, D., Dieu-Nosjean, M.-C., Validire, P., Trautmann, A., Mami-Chouaib, F., and Donnadieu, E. (2012) Matrix architecture defines the preferential localization and migration of T cells into the stroma of human lung tumors. *J. Clin. Invest.* **122**, 899–910

Received for publication July 10, 2018.
Accepted for publication November 5, 2018.